The Role of PCSK9 in Glomerular Lipid Accumulation and Renal Injury in Diabetic Kidney Disease

Chang-Yun Yoon

Department of Medicine
The Graduate School, Yonsei University

The Role of PCSK9 in Glomerular Lipid Accumulation and Renal Injury in Diabetic Kidney Disease

Directed by Professor Tae-Hyun Yoo

The Doctoral Dissertation
submitted to the Department of Medicine,
the Yonsei University Graduate School of Medicine
in partial fulfillment of the requirements for the degree of
Doctor of Philosophy

Chang-Yun Yoon

June 2019

This certifies that the Doctoral Dissertation
of Chang–Yun Yoon is approved.

Thesis Supervisor: Tae–Hyun Yoo

Thesis Committee Member #1: Shin–Wook Kang

Thesis Committee Member #2: Dong–Ryeol Ryu

Thesis Committee Member #3: Sung Ha Park

Thesis Committee Member #4: Min Jung Chang

The Graduate School
Yonsei University

June 2019

ACKNOWLEDGEMENTS

I would like to thank Professor Tae–Hyun Yoo, who is a mentor of life and a professor of doctoral degree, for leading me from the beginning until the completion of the doctoral course. I was thoughtfully taught about the extensive and in–depth review process through the logical approach to complex life science. In addition, I would like to express my deepest gratitude and appreciation to Professor Shin–Wook Kang, who is the chairman of the examination committee of my doctoral degree and eternal master, for his endless support for both education and research. I would also like to extend my gratitude to Dong–Ryeol Ryu, Sung Ha Park, and Min Jung Chang for their thoughtful consideration and sharp teaching. I am grateful to Professor Seung–Hyeok Han, who gave a lot of support and encouragement to me as a good example of deep and meticulous researcher and a great educator. I would like to express my heartfelt gratitude to Professor Jung Tak Park for his devoted teaching and affection with his passion, which was endlessly lacking. I would like to express my deep gratitude to Jimin Park for her efforts and sacrifices, and to Professor Meiyan Wu. I would also like to thank Dr. Bo Young Nam and Dr. Seonghun Kim for their kind support during the experiments. Although I did not mention it here, I am deeply grateful to all those who have shown a lot of help and affection in the doctoral program. I think it was very extravagant luck that I could have enjoyed the opinions of professors, seniors, and colleagues who had overwhelming logic and excellent personality. I sincerely hope that the results and insights we have shown in my doctoral dissertation have contributed to the truth of the life sciences that we intend to achieve. Finally, I would like to say that I love my family, who have shown me a resting place and unchanging faith that I can always return to.

TABLE OF CONTENTS

LIST OF FIGURES

LIST OF TABLES

ABSTRACT

The Role of PCSK9 in Glomerular Lipid Accumulation and Renal Injury in Diabetic Kidney Disease

Chang–Yun Yoon

Department of Medicine
Yonsei University Graduate School of Medicine

(Directed by Professor Tae–Hyun Yoo)

Background: Glomerular lipid accumulation is one of the pathologic characteristics of diabetic kidney disease (DKD). Recent evidences have suggested the specific role of proprotein convertase subtilisin/kexin type 9 (PCSK9) in cellular lipid homeostasis. Herein, I evaluate the role of PCSK9 in lipid accumulation in glomeruli and podocytes under diabetic condition.

Methods: C57BL/6 and PCSK9 knockout mice were fed with high fat diet and intraperitoneally injected with low dose streptozotocin for 12 weeks. Lipid accumulation in the kidney tissue was confirmed with BODIPY 493/503 staining. Upregulation or downregulation of PCSK9 expression in mouse podocytes was mediated by lentivirus or small–interfering RNA (siRNA) in the presence of various treatments. Apoptosis, mitochondrial morphology, and the key factors related to energy metabolism were evaluated both *in vivo* and *in vitro*.

Results: Lipid accumulation was significant in the kidney tissues from DKD with PCSK9 knockout as compared to control and DKD only mice. Mitochondrial morphology and the expression of metabolic enzymes were disturbed in PCSK9 knockout mice. Intracellular lipid accumulation and apoptosis along with mitochondrial swelling and crista disruption increased in the podocytes after treatment. These changes ameliorated after PCSK9 overexpression but

aggravated after siRNA–medicated knockdown of PCSK9 expression.

Conclusion: These findings suggest that PCSK9 down–regulation in podocytes may be related to lipid accumulation and renal injury through mitochondrial dysfunction and apoptosis in DKD.

Key words: PCSK9, lipid accumulation, podocyte, mitochondria, diabetic kidney disease

The Role of PCSK9 in Glomerular Lipid Accumulation and Renal Injury in Diabetic Kidney Disease

Chang–Yun Yoon

Department of Medicine
Yonsei University Graduate School of Medicine

(Directed by Professor Tae–Hyun Yoo)

I. INTRODUCTION

Glomerular lipid accumulation is one of the pathologic characteristics of diabetic kidney disease (DKD). Kimmelstiel and Wilson first reported the presence of lipid droplets in the kidney of patient with DKD.[1] Resent studies have revealed the existence of lipid accumulation in the podocyte foot process.[2] Lipid overload in the kidneys was also reported in various experimental models of DKD. Renal triglyceride and cholesterol accumulation were observed in Akita and OVE26 mice, a typical DKD model of type 1 diabetes.[3] In addition, renal lipid accumulation was observed in the glomeruli and tubules of both type 2 DKD animal models, FVB$^{db/db}$ and BTBR *ob/ob* mice.[4,5]

Proprotein convertase subtilisin/kexin type 9 (PCSK9) is a soluble member of the mammalian proprotein convertase family of secretory serine endoprotease. PCSK9 is mainly synthesized and secreted by the liver and intestine, but is also expressed in the kidney and brain.[6] PCSK9 was shown to be related to the circulation of low–density lipoprotein cholesterol (LDL–C).[7] The gain–of–function mutation (D374Y) or overexpression of PCSK9 causes severe

hypercholesterolemia and profound atherosclerotic lesion in mice.[8,9] These results have highlighted the function of PCSK9, wherein PCSK9 binds to the LDL–C receptor (LDLR) and promotes the degradation of LDLR essential for LDL–C clearance.[10] As a result, a drug molecule that ameliorates cardiovascular diseases by targeting PCSK9 was developed and is currently being used in clinical practices.[11-14] PCSK9 also plays a role in triglyceride metabolism, although the exact mechanism is incompletely understood. Hypertriglyceridemia and increased hepatic triglyceride–rich–lipoprotein outputs were observed in mice with systemic overexpression of PCSK9 and transgenic expression of PCSK9–D374Y.[15,16]

Further in–depth studies on PCSK9 have revealed its involvement in intracellular lipid homeostasis through several pathways in various tissues. PCSK9 maintains cellular lipid homeostasis by regulating cholesterol levels as well as by influencing the storage and secretion of triglycerides in the epithelial cells of the intestine.[17,18] In addition, adipocyte hypertrophy was observed through lipid accumulation in PCSK9 knockout (KO) mice, wherein PCSK9 was shown to be involved in the cellular metabolism of long–chain fatty acids.[19,20] PCSK9 induces degradation of CD36, a major receptor that controls fatty acid and triglyceride metabolism.[20] Interestingly, there is also a link to molecular biologic responses that are thought to be less relevant to lipid regulation. Lipopolysaccharide–stimulated vascular smooth muscle cell (VSMC) releases and enhances PCSK9, and there may be bidirectional interplay between PCSK9 and mitochondrial DNA damage in VSMC.[21] There is also a report that PCSK9 expression is associated with apoptosis in human umbilical vein endothelial cells.[22] However, the above–mentioned changes associated with PCSK9 expression have not been studied in kidney tissues and cells.

I investigated the role of PCSK9 in the regulation of lipid accumulation and homeostasis in glomeruli and podocytes under diabetic conditions. Furthermore, I aimed to identify the pathophysiology of podocyte injury responsible for

PCSK9–induced lipid accumulation in DKD.

II. MATERIALS AND METHODS

1. Human study

The human samples and demographic data were obtained from the Yonsei Renal cDNA Bank following the guidelines of the respective local ethics committees. Of 102 samples diagnosed, 32 and 50 samples were confirmed with DKD and IgA nephropathy (IgAN), respectively, while 20 normal samples were used as controls. The biochemical analyses were performed in an accredited hospital laboratory (Yonsei University Health System, Seoul, Republic of Korea). Informed consent was obtained from all patients. The biopsy tissue specimens were manually micro–dissected,[23,24] and glomerular gene expression profiling was performed as previously described.[5]

2. Animal study

Male C57BL/6J mice, two sets of heterozygous PCSK9 KO, and *db/db* mice were purchased from The Jackson Laboratory (Bar Harbor, ME, USA). After homozygous mating, appropriate animals were selected by genotyping. The animals were maintained in a temperature–controlled room (22°C) in a 12–hr light/dark cycle. One week after arrival, C57BL/6J mice (5 weeks old) were divided into two groups and fed with either normal diet (wild type, WT; $n = 10$) or high fat diet (HFD, WT HFD; $n = 20$) for up to 16 weeks. PCSK9 KO mice (KO HFD; $n = 20$) fed the same HFD as WT mice. I refer to previous studies that produced a type 2 diabetes mellitus animal model combining HFD and low–dose streptozotocin administration.[25,26] During the first 4 weeks, only HFD was administered to induce insulin resistance, while a low–dose of streptozotocin (50 mg/kg each day) was injected during the subsequent 12 weeks to maintain hyperglycemia for 3 consecutive days every 6 weeks. The HFD (Research Diets, New Brunswick, NJ, USA) comprised 60% fats from lard, 20% carbohydrates,

and 20% proteins, whereas the normal diet contained 12% fats, 64.5% carbohydrates, and 23.5% proteins. Body weight and blood glucose level (blood collected through tail vein) were measured once every 2 weeks. Mice from different groups were subjected to metabolic cage analysis after the completion of experiment time. Mice were sacrificed and perfused with saline, while the blood was directly collected from the heart. Following immediate centrifugation of blood samples at 4°C, plasma was separated and stored at –20°C until analysis. The kidney tissues were sampled for different analyses. Glomeruli were isolated by a sieving technique. Glomeruli were collected under an inverted microscope, and tubular sections were stored separately. Purity of the glomerular preparation was greater than 98% as determined by light microscopy.

The protocols for animal experiments were approved by the Committee for the Care and Use of Laboratory Animals at Yonsei University College of Medicine in Seoul, Republic of Korea (No. H14C2003). All experiments with animals were conducted in accordance with the Principles of Laboratory Animal Care (NIH Publication no. 85–23, revised 1985).

3. Podocyte cultures, CMV–mPCSK9–lentivirus (Lv–PCSK9) infection, and small–interfering RNA (siRNA) transfection

Conditionally immortalized mouse podocytes were kindly provided by Dr. Peter Mundel (Founder, Senior Vice President of Biology and Advisor, Goldfinch Biopharma Inc., Cambridge, MA, USA) and were cultured as previously described.[27] Frozen podocytes were first cultured under permissive conditions in collagen–coated 100–mm plates with Roswell Park Memorial Institute (RPMI)–1640 medium (Sigma–Aldrich, UK) containing 10% fetal bovine serum (Gibco, Thermo Fisher Scientific, Waltham, MA, USA), 10 U/mL interferon–γ, and 100 U/mL penicillin G (Sigma–Aldrich, UK) at 33°C for 4–5 days, then subcultured and transferred in a complete medium without interferon–γ at 37°C for another 10–12 days. The differentiation of podocytes was confirmed by the detection of

synaptopodin, a podocyte differentiation marker, by reverse transcriptase–polymerase chain reaction (RT–PCR) and Western blotting.

Lentivirus production was performed according to previous studies.[28,29] Briefly, human embryonic kidney (HEK) 293FT cells (Invitrogen, Carlsbad, CA, USA) seeded in 150 mm plates were transfected with 2.5 μg of Lv–PCSK9 using Lenti–Pac™ HIV kit (GeneCopoeia, USA). After 48 hr, supernatants were collected, centrifuged at 500 *g* for 10 min and filtered through a 0.45 μm filter. Next, transfer clarified supernatant to a sterile container and combine 1 volume of Lenti–X Concentrator (TaKaRa, CA, USA) with 3 volumes of clarified supernatant. And the samples were centrifuged at 1,500 *g* for 90 min, and the resulting pellet was resuspended in phosphate buffer saline (PBS). Lentivirus titer was determined by transfecting HEK 293FT cells with a dilution series of the viral suspension. Lentivirus samples at a titer of 4×10^6 transfection units (TU)/mL were stored at –80°C. A total of 4×10^5 TU/mL of lentivirus suspension containing Lv–PCSK9 was added to the cultured cells. After 8–12 hr, the media were changed to routine culture media.

At the same time, I down-regulated intracellular *PCSK9* expression using siRNA against mouse *PCSK9*. *PCSK9* siRNA (siPCSK9) was transiently transfected into differentiated podocytes for 24 hr, and this procedure was performed using Lipofectamine 2000 (Invitrogen, Carlsbad, CA, USA).

For *in vitro* studies, depending on the purpose of the experiments, cells were incubated with 5 ng/mL TNF–α (Roche, Switzerland) for 12 hr and 100 μM palmitic acid (PA; Sigma–Aldrich, UK) for 48 hr.

4. Urinary albumin and creatinine measurement

Urine was collected for 24 hr using a metabolic cage and immediately centrifuged at 4°C. The supernatant was obtained and used for analysis. Urinary albumin and creatinine were diluted with different dilution factors. Urine albumin was measured using a commercially available kit (Exocell, Inc., Philadelphia, PA,

USA) according to the manufacturer's instructions and urine creatinine was measured by Seoul Clinical Laboratories (Seoul, Republic of Korea).

5. Cholesterol and triglyceride assays

Serum cholesterol and triglyceride were measured by Seoul Clinical Laboratories (Seoul, Republic of Korea). A total of 4×10^6 podocytes and 10 mg of kidney cortex tissues per animal from different groups were used for total cholesterol and triglyceride measurements using cholesterol and triglyceride assay kit (Cayman Chemical, Ann Arbor, MI, USA), respectively. In short, the cells or kidney tissues were suspended in chloroform / isopropanol / NP–40 (7:11:0.1) mixture, homogenized, and centrifuged at room temperature and 15,000 *g*. The supernatants were collected in new EP tubes and incubated at 50°C until the evaporation of the buffer, followed by dilution with an assay buffer before analysis using the kits.

6. Total RNA extraction

Total RNA was extracted from mouse kidney as previously described.[30] Whole kidney samples were rapidly frozen using liquid nitrogen and homogenized by mortar and pestle thrice with 700 μL of RNA STAT–60 reagent (TaKaRa, CA, USA). After homogenizing the suspension for 5 min at room temperature, 160 μL of chloroform was added. Next, the mixture was shaken vigorously for 30 sec, incubated for 10 min at ice, and centrifuged at 12,000 *g* for 15 min at 4°C. The upper aqueous phase containing the extracted RNA was transferred to a new tube. RNA was precipitated from the aqueous phase by adding 400 μL of isopropanol, and then pelleted by centrifugation at 12,000 *g* for 30 min at 4°C. The RNA precipitate was washed with 70% ice–cold ethanol, air dried for 10 min, and dissolved in diethyl pyrocarbonate (DEPC)–treated distilled water. RNA yield and quality were assessed based on spectrophotometric measurements at wavelengths of 260 and 280 nm. Total RNAs from cultured podocyte cells were

extracted similarly.

7. Reverse transcription

First strand cDNA was made by using a Boehringer Mannheim cDNA synthesis kit (Boehringer Mannheim GmbH, Mannheim, Germany). Two micrograms of total RNA extracted from tissues and cultured cells were reverse transcribed using 10 μM random hexanucleotide primer, 1 mM dNTP, 8 mM $MgCl_2$, 30 mM KCl, 50 mM Tris·HCl, pH 8.5, 0.2 mM dithiothreithol, 25 U RNAse inhibitor, and 40 U AMV reverse transcriptase. The mixture was incubated at 30°C for 10 min and 42°C for 1 hr, followed by inactivation of the enzyme at 99°C for 5 min.

8. Real–time quantitative polymerase chain reaction (qPCR)

I compared the transcript levels of mouse or human *PCSK9*, peroxisome proliferator–activated receptor gamma coactivator 1–alpha *(Ppargc1a),* and the genes related to β–oxidation and apoptosis by qPCR. The RNAs used for amplification were 25 ng per reaction tube. Using the ABI PRISM 7700 Sequence Detection System (Applied Biosystems, Foster City, CA, USA), a total volume of 20 μL mixture in each well was used containing 10 μL of SYBR Green PCR Master Mix (Applied Biosystems, Foster City, CA, USA), 5 μL of cDNA, and 5 pmol sense and antisense primers. The sequences of primers are presented in **Table 1**. The PCR conditions were as follows: 35 cycles of denaturation for 30 min at 94.5°C, annealing for 30 sec at 60°C, and extension for 1 min at 72°C. Initial heating for 9 min at 95°C and final extension for 7 min at 72°C were performed for all PCR reactions. Each sample was run in triplicate in separate tubes, and a control without cDNA was also run in parallel with each assay. After real–time PCR, the temperature was increased from 60 to 95°C at a rate of 2°C /min to construct a melting curve. The cDNA content of each specimen was determined using a comparative C_T method with $2^{-\Delta\Delta CT}$. The results were given as the relative expression normalized to the expression of 18s rRNA and

expressed in arbitrary units.

Table 1. Sequences of oligonucleotide primers used for qPCR test

Genes		Sequences
PCSK9	**Forward**	CAGAGGTCATCACAGTCGGG
	Reverse	GGGGCAAAGAGATCCACACA
LDLR	**Forward**	AGCCATTTTCAGTGCCAATC
	Reverse	TGTGACCTTGTGGAACAGGA
CD36	**Forward**	TGCTGGAGCTGTTATTGGTG
	Reverse	TGGGTTTTGCACATCAAAGA
NPHS1	**Forward**	AGAACTTGCCACCTGATTCC
	Reverse	CCTTCCACCACAGTCAGGTTT
NPHS2	**Forward**	TTGCACACTCTTCAGTCGCT
	Reverse	GATGCTCCCTTGTGCTCTGT
Cpt1	**Forward**	GGTCTTCTCGGGTCGAAAGC
	Reverse	TCCTCCCACCAGTCACTCAC
Ppargc1a	**Forward**	AGTCCCATACACAACCGCAG
	Reverse	CCCTTGGGGTCATTTGGTGA
Acox1	**Forward**	CTTGGATGGTAGTCCGGAGA
	Reverse	TGGCTTCGAGTGAGGAAGTT
Bcl–2	**Forward**	TGGGATGCCTTTGTGGAACT
	Reverse	CAGCCAGGAGAAATCAAACAGA
Bax	**Forward**	TCCACCAAGAAGCTGAGCGAG
	Reverse	GTCCAGCCCATGATGGTTCT
18s	**Forward**	AACTAAGAACGGCCATGCAC
	Reverse	CCTGCGGCTTAATTTGACTC

9. Western blot analyses

Protein expression levels of mouse PCSK9 and apoptosis markers were examined with Western blot analyses. All experiments were performed in triplicate. I prepared cell lysates in radioimmunoprecipitation assay (RIPA) lysis buffer supplemented with a protease inhibitor cocktail (Roche, Switzerland) and phosphatase inhibitor (Roche, Switzerland). Proteins were resolved by electrophoresis on 5–15% acrylamide denaturing SDS–polyacrylamide gels,

transferred onto nitrocellulose or polyvinylidene difluoride membranes, and probed with the antibodies against the following proteins: PCSK9, CD36 (Abcam, Cambridge, MA, USA), LDLR (R&D Systems, Minneapolis, MN, USA), PGC–1α (Abcam, Cambridge, MA, USA), Bax (Santa Cruz Biotechnology, Santa Cruz, CA, USA), B cell lymphoma–2 (Bcl–2; Santa Cruz Biotechnology, Santa Cruz, CA, USA), cleaved–caspase 3 (Cell Signaling Technology, Danvers, MA, USA), and β–actin (Sigma–Aldrich, UK). A horseradish peroxidase (HRP)–conjugated anti–rabbit (Cell Signaling Technology, Danvers, MA, USA) or anti–mouse IgG antibody (Cell Signaling Technology, Danvers, MA, USA) were used as secondary antibodies. After frequent rinses, the membranes were developed by chemiluminescence (Thermo Fisher Scientific, Waltham, MA, USA). To quantify the band densities, I used ImageJ software ver. 1.49 (National Institutes of Health, Bethesda, MD; online at http://rsbweb.nih.gov/ij).

10. Histology, immunohistochemistry, and lipid droplet staining

For histological evaluation, formalin–fixed, paraffin–embedded kidney sections were stained with periodic acid–Schiff (PAS). To fix the kidney sample, 10% neutral–buffered formalin was used. Paraffin–embedded tissues were processed in 5 μm–thick sections for immunohistochemical staining. Tissue sections were deparaffinized, rehydrated in ethyl alcohol, and washed in tap water. Antigen retrieval was performed in 10 mM sodium citrate buffer for 20 min using a Black & Decker vegetable steamer. Slides were blocked with 10% donkey serum for 30 min at room temperature and then washed using PBS. A anti–PCSK9, anti–CD36 (Abcam, Cambridge, MA, USA), and anti–LDLR (R&D Systems, Minneapolis, MN, USA) antibodies were diluted to a proper concentration with 2% casein in bovine serum albumin, and then incubated overnight at 4°C. After washing, a secondary goat anti–rabbit antibody (Agilent, CA, USA) was added for 1 hr at room temperature. Diaminobenzidine was added for 2 min, hematoxylin was used to counterstain the slides.

For lipid droplet staining, 20 μm–thick cryosections and stimulated mouse podocytes cultured in chambers were fixed with 4% paraformaldehyde for 10 min, washed thrice with PBS, and incubated for 60 min at room temperature with 5 μg/mL of fluorescent neutral lipid stain BODIPY 403/503 (Life Technologies Corp., Carlsbad, CA, USA). After washing, the sections and podocytes were counterstained with 4′,6–diamidino–2–phenylindole (DAPI) and mounted with Vectashield (Vector Laboratories, Burlingame, CA, USA).

11. Terminal deoxynucleotidyl transferase dUTP nick-end labeling (TUNEL) assay

Apoptosis was evaluated by TUNEL assay using a commercially available kit (Millipore, Burlington, MA, USA). TUNEL–positive glomerular cells in formalin–fixed renal tissues were identified by examining at least 30 glomeruli at ×40 magnification.

12. Electron microscopic examination

Podocyte foot effacement, mitochondrial structure, and lipid drops in the kidney tissues were examined with transmission electron microscopy (TEM). A total of 1×10^6 mouse podocytes and 1×1 mm^3 kidney cortex tissues were fixed for 12 hr in 2% Glutaraldehyde–Paraformaldehyde in 0.1M phosphate buffer (pH 7.4) and washing in 0.1M phosphate buffer. They were post–fixed with 1% OsO4 dissolved in 0.1M phosphate buffer for 2 hr and dehydrated in ascending gradual series (50–100%) of ethanol and infiltrated with propylene oxide. Specimens were embedded by Poly/Bed 812 kit (Polysciences, Inc., PA, USA). After pure fresh resin embedding and polymerization at 65°C electron microscope oven (TD–700, DOSAKA, Japan) for 24 hr. Sections about 200–250 nm–thin were initially cut and stained with toluidine blue (Sigma–Aldrich, UK) for light microscope. For contrast staining, 70 nm thin sections were double stained with 6% uranyl acetate for 20 min (Electron Microscopy Sciences MS, Hatfield, PA, USA) and lead citrate for 10 min (Thermo Fisher Scientific, Waltham, MA, USA).

There sections were cut by LEICA EM UC–7 (Leica Microsystems, Austria) with a diamond knife (Diatome, Bienne, Switzerland) and transferred on copper and nickel grids. All thin sections were observed by TEM (JEM–1011, JEOL, Japan) at the acceleration voltage of 80 kV.

13. Statistical analyses

Statistical analyses were performed using IBM SPSS software for Windows version 23.0 (IBM Corporation, Armonk, NY, USA). Continuous variables are presented as mean ± standard deviation, and categorical variables are shown as numbers (percentage). To analyze differences between two groups, Mann–Whitney U test was used, and Kruskal–Wallis test was applied for comparison between more than two groups. For all analyses, $P < 0.05$ was considered statistically significant.

III. RESULTS

1. Renal expression of PCSK9 decreases in DKD

In animal model, the levels of PCSK9 in the kidney samples from *db/db* mice showed that the transcription and expression levels of PCSK9 significantly decreased than *db/m* mice (**Fig. 1A–C**).

The transcription level of *PCSK9* was examined in the tissue samples obtained from the patients with renal disease. The clinical characteristics of patients are shown in **Table 2**. Patients with DKD were older than those with normal kidney function or IgAN, and their estimated glomerular filtration rate was significantly decreased. Proteinuria and circulating cholesterol levels were higher in the patients with IgAN and DKD than control subjects. No difference was observed in the transcription levels of *PCSK9* between IgAN and the control group, but it was significantly reduced in patients with DKD as compared to control or IgAN groups (control vs. DKD, $P < 0.01$; IgAN vs. DKD, $P < 0.01$; **Fig. 1D**).

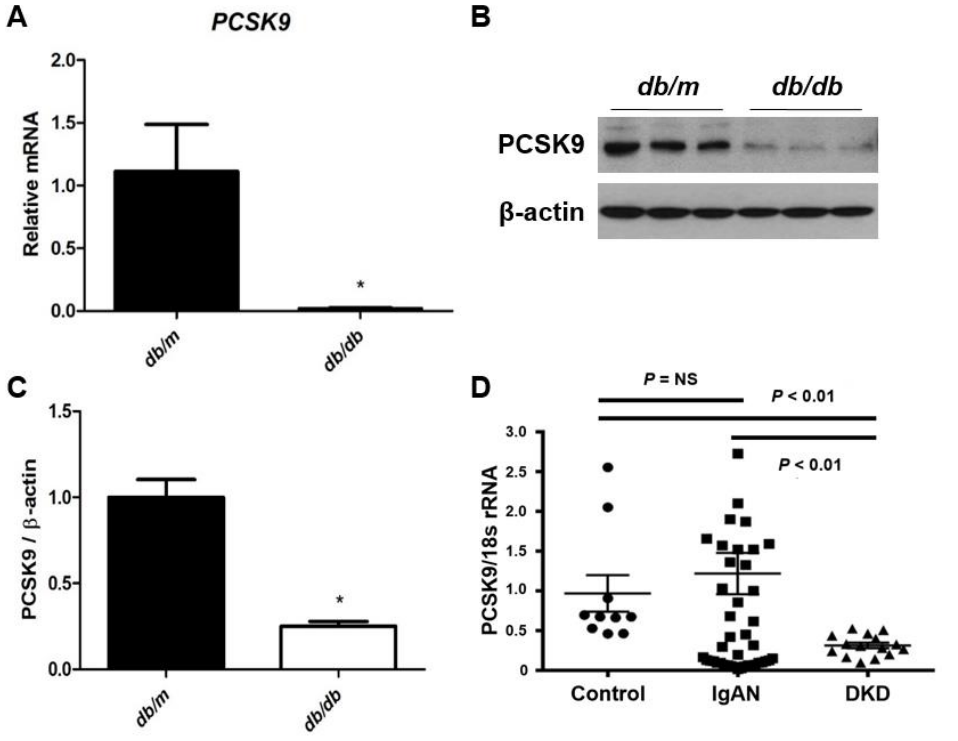

Figure 1. Decreased renal expression of PCSK9 in the glomeruli of human kidneys with DKD and the kidneys of type 2 diabetic mice. (A–C) PCSK9 mRNA and protein levels in the kidneys from *db/m* and *db/db* mice. **(D)** PCSK9 mRNA expression in glomerular samples from patients with control (n = 20), IgAN (n = 50), and DKD (n = 32).

Note: *, $P < 0.05$ vs. *db/m*.

Abbreviations: PCSK9, proprotein convertase subtilisin/kexin type 9; NS, not significant; IgAN, IgA nephropathy, DKD, diabetic kidney disease.

Table 2. Clinical characteristics of patients

Variables	Control (*n* = 20)	IgAN (*n* = 50)	DKD (*n* = 32)	*P*
Age (years)	23.8 ± 10.9	39.1 ± 11.7	51.7 ± 12.5	<0.001
Male (*n*, %)	18 (90)	16 (32)	22 (69)	<0.001
BUN (mg/dL)	12.4 ± 2.9	14.9 ± 4.5	36.2 ± 15.7	<0.001
Creatinine (mg/dL)	0.9 ± 0.2	0.9 ± 0.3	3.0 ± 2.2	<0.001
eGFR (mL/min/1.73 m^2)	116 ± 18	91 ± 23	36 ± 26	<0.001
Cholesterol (mg/dL)	160 ± 33	196 ± 43	200 ± 65	0.001
Triglyceride (mg/dL)	98 ± 41	146 ± 111	195 ± 113	0.005
HDL–C (mg/dL)	50 ± 7	54 ± 15	50 ± 22	0.87
LDL–C (mg/dL)	81 ± 25	118 ± 36	112 ± 44	0.04
UPCR (g/g Cr)	0.26 ± 0.31	1.79 ± 1.38	8.13 ± 5.40	<0.001
UACR (mg/g Cr)	201 ± 277	1374 ± 1060	5393 ± 3950	<0.001

Abbreviations: IgAN, IgA nephropathy; DKD, diabetic kidney disease; BUN, blood urea nitrogen; eGFR, estimated glomerular filtration rate; HDL–C, high–density lipoprotein cholesterol; LDL–C, low–density lipoprotein cholesterol; UPCR, urine protein to creatinine ratio; UACR, urine albumin to creatinine ratio.

2. The decrease of PCSK9 is associated with renal lipid accumulation and injury in DKD model

To investigate the role of PCSK9 in type 2 DKD, I generated DKD models through HFD and streptozotocin treatment in WT or PCSK9 KO animals and compared results with the control group. First, I confirmed that type 2 diabetes is induced in animal models that have undergone HFD and low–dose streptozotocin injection. The body weight and random blood glucose were significantly increased in WT HFD and KO HFD groups than in control mice (**Fig. 2A**). Then, PCSK9 levels were identified in KO HFD mice. In comparison with the WT group, WT HFD mouse kidneys showed a significant decrease in the transcription and expression of PCSK9, which further decreased in the kidney samples from KO HFD mice (**Fig. 2B–D**). This trend was confirmed in immunohistochemistry for PCSK9 (**Fig. 2E**).

The lipid changes were measured in the kidneys of the animal models generated by the previous method. First, circulating cholesterol levels that were elevated in the WT HFD group compared to the WT, and these were offset in KO HFD group (**Fig. 3A**). On the other hand, the levels of total cholesterol and triglycerides in the kidney tissues were significantly higher in WT HFD group than in WT group, but the highest levels were reported in KO HFD group (**Fig. 3B**). In addition, BODIPY 493/503 stain showed that lipid accumulation occurred most in the kidneys from KO HFD group (**Fig. 3C**). In order to confirm the mechanism of lipid accumulation in kidney, I examined how LDLR and CD36 expression changes according to the expression of PCSK9. I could observe that both transcription and expression of CD36 and LDLR were increased in the order of WT, WT HFD, and KO HFD group (**Fig. 4A–C)**. The same trend was also observed for immunohistochemistry staining against CD36 and LDLR (**Fig. 4D**).

Next, I examined whether changes of PCSK9 in DKD animal models were associated with renal injury. PAS stain findings showed that increase in glomerulus size and mesangial expansion were most prominent in KO HFD model. In addition, foot process effacement of podocyte was the most severe in KO HFD (**Fig. 5A**). Furthermore, albuminuria tended to gradually deteriorate in the WT, WT HFD, and KO HFD groups (**Fig. 5B**). I also evaluated podocyte injury with several parameters, including *NPHS1* and *NPHS2* transcription levels. The decrease in *NPHS1* and *NPHS2* transcript levels was most severe in KO HFD group (**Fig. 5C**). All these findings suggest that decreased PCSK9 expressions were associated with renal lipid accumulation and injury in DKD animal model.

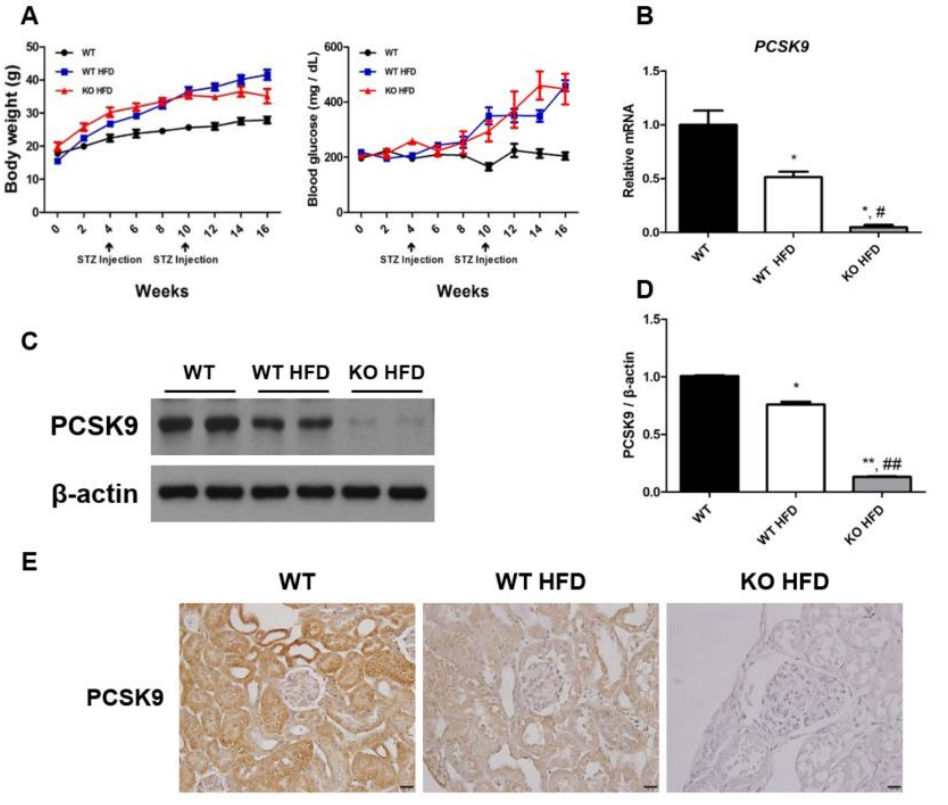

Figure 2. The expression of PCSK9 is decreased in DKD animal model. (A) Body weight and random blood glucose in WT (n = 10), WT HFD (n = 20), and PCSK9 KO HFD mice (n = 20). **(B–D)** The transcription (B) and expression (C and D) levels of PCSK9 in the kidney of animal models. **(E)** Immunohistochemistry staining of PCSK9 for the kidneys of animal models.

Note: *, $P < 0.05$ vs. WT; **, $P < 0.001$ vs. WT; #, $P < 0.05$ vs. WT HFD; ##, $P < 0.001$ vs. WT HFD.

Abbreviations: WT, wild type; HFD, high fat diet; KO, knockout; STZ, streptozotocin; PCSK9, proprotein convertase subtilisin/kexin type 9; DKD, diabetic kidney disease.

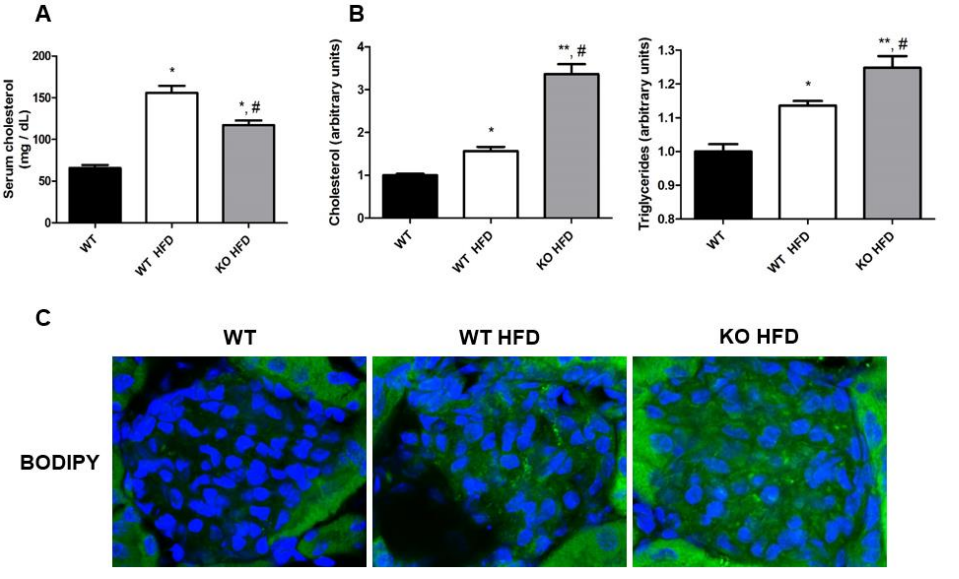

Figure 3. Decreased PCSK9 expression aggravates lipid accumulation in the kidneys of type 2 DKD mice. (A) Serum total cholesterol in animal models. **(B)** Total cholesterol and triglyceride levels in the kidneys from animal models. **(C)** BODIPY staining of the kidneys from animal models.

Note: *, $P < 0.05$ vs. WT; **, $P < 0.001$ vs. WT; #, $P < 0.001$ vs. WT HFD.

Abbreviations: WT, wild type; HFD, high fat diet; KO, knockout.

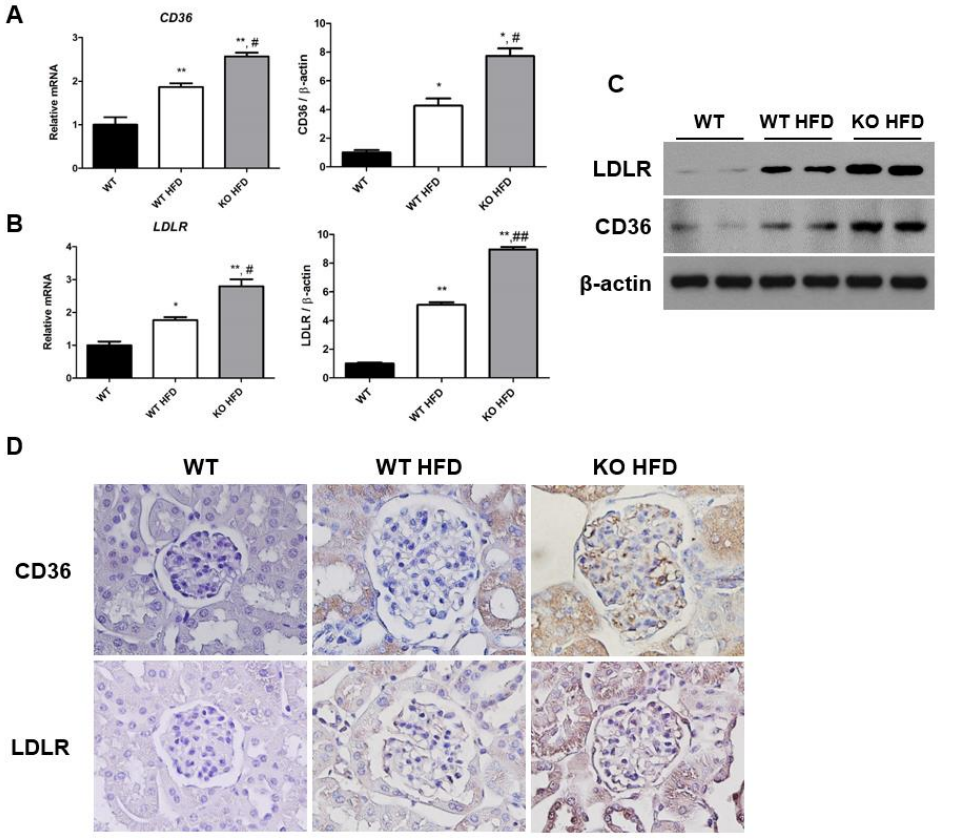

Figure 4. Increased expression of CD36 and LDLR in PCSK9 KO animal models. (A–C) Transcriptions and expressions of CD36 and LDLR in animal models. **(D)** Immunohistochemical staining for CD36 and LDLR in animal models.

Note: *, $P < 0.05$ vs. WT; **, $P < 0.001$ vs. WT; #, $P < 0.05$ vs. WT HFD; ##, $P < 0.001$ vs. WT HFD.

Abbreviations: WT, wild type; KO; knockout; LDLR, low–density lipoprotein cholesterol receptor.

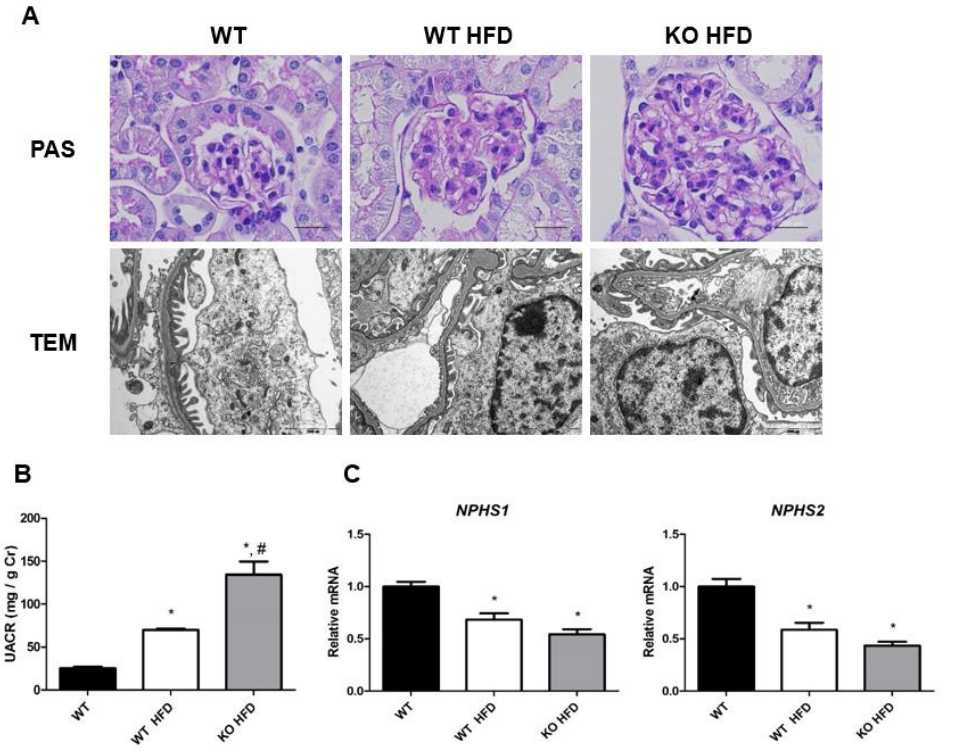

Figure 5. Decrease PCSK9 is associated with renal injury in DKD animal model. (A) PAS staining and TEM for kidney samples from WT, WT HFD, and KO HFD animal models. **(B)** UACR for mice from different animal models. **(C)** *NPHS1* and *NPHS2* mRNA levels in the kidney samples from different experimental groups.

Note: *, $P < 0.001$ vs. WT; #, $P < 0.05$ vs. WT HFD.

Abbreviations: WT, wild type; HFD, high fat diet; KO, knockout; PAS, periodic acid–Schiff; TEM, transmission electron microscope; UACR, urine albumin to creatinine ratio; PCSK9, proprotein convertase subtilisin/kexin type 9; DKD, diabetic kidney disease.

3. Downregulated PCSK9 expression exacerbates the alteration of mitochondrial morphology and fatty acid oxidation in animal DKD model

In according to a previous study that has shown that mitochondrial damage and

fatty acid oxidation are involved in the lipid accumulation and renal injury in DKD,[31,32] the related surrogate markers were examined. The levels of PGC–1α levels, a key regulator of mitochondrion biogenesis and energy metabolism, were evaluated in the kidneys from three different experimental groups. The transcription and expression of *PGC–1α* in the kidney tissues significantly decreased in WT HFD and KO HFD groups (**Fig. 6A–C**). In addition, the key enzymes involved in fatty acid oxidation such as *carnitine palmitoyltransferase–1* (*Cpt1*) and *acyl–CoA oxidase* (*Acox1*) mostly reduced in KO HFD group (**Fig. 6D and E**). TEM imaging revealed edema and partial disappearance of cristae in the mitochondria from WT HFD podocytes, and these changes were more prominent in KO HFD group (**Fig. 6F**).

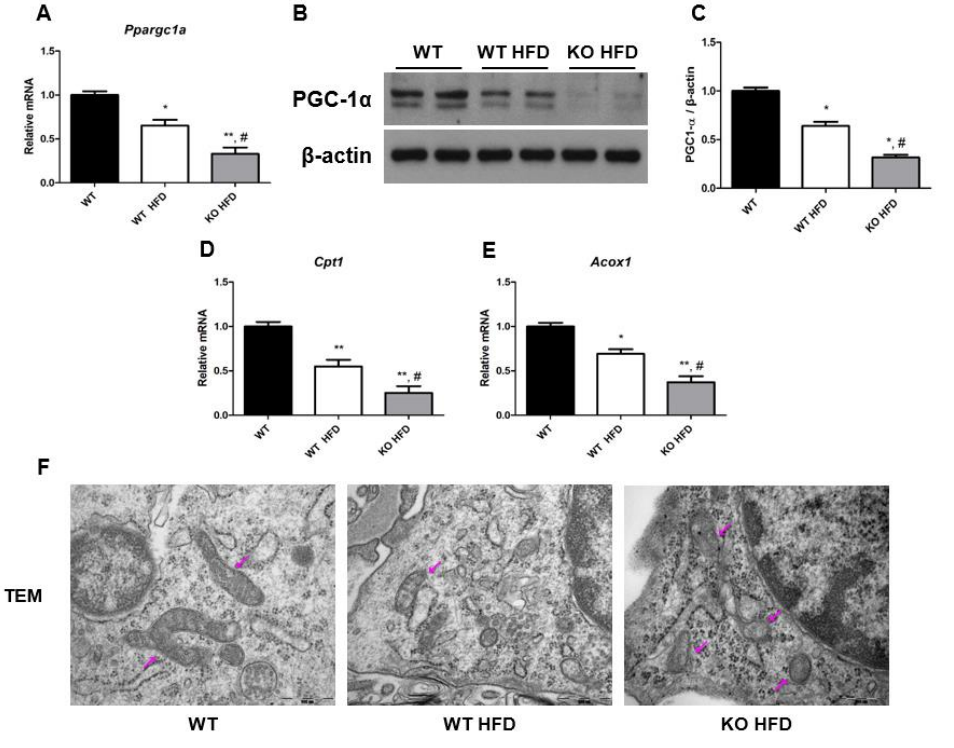

Figure 6. PCSK9 downregulation is associated with the alteration in mitochondrial morphology and fatty acid oxidation in DKD model. (A–C) Transcription (A) and expression (B and C) of PGC–1α in the kidney tissues from animal models. **(D and E)** The transcription levels of *Cpt1* and *Acox1* in the samples obtained from different animal models. **(F)** Glomerulus findings of animal models taken by TEM.

Note: *, $P < 0.05$ vs. WT; **, $P < 0.001$ vs. WT; #, $P < 0.05$ vs. WT HFD. **Abbreviations:** WT, wild type; HFD, high fat diet; KO, knockout; PGC–1α, peroxisome proliferator–activated receptor gamma coactivator 1–alpha; Cpt1, carnitine palmitoyltransferase–1; Acox1, acyl–CoA oxidase; TEM, transmission electron microscope; PCSK9, proprotein convertase subtilisin/kexin type 9; DKD, diabetic kidney disease.

4. Decreased PCSK9 expression associates with apoptosis in DKD animal model

I investigated whether the decrease in PCSK9 expression was associated with apoptosis, the most common type of cell death in DKD. The mRNA levels of *Bcl–2*, an anti–apoptotic protein, were in the order of WT > WT HFD > KO HFD groups, while the expression levels of Bax and the ratio of Bax to Bcl–2, apoptotic markers, increased in an inverse order (**Fig. 7A–C**). In addition, cleaved–caspase 3 levels, another apoptotic marker, increased in WT HFD and KO HFD groups as compared with WT group (**Fig. 7A and D**). This trend was confirmed again in the TUNEL assay (**Fig. 7E**).

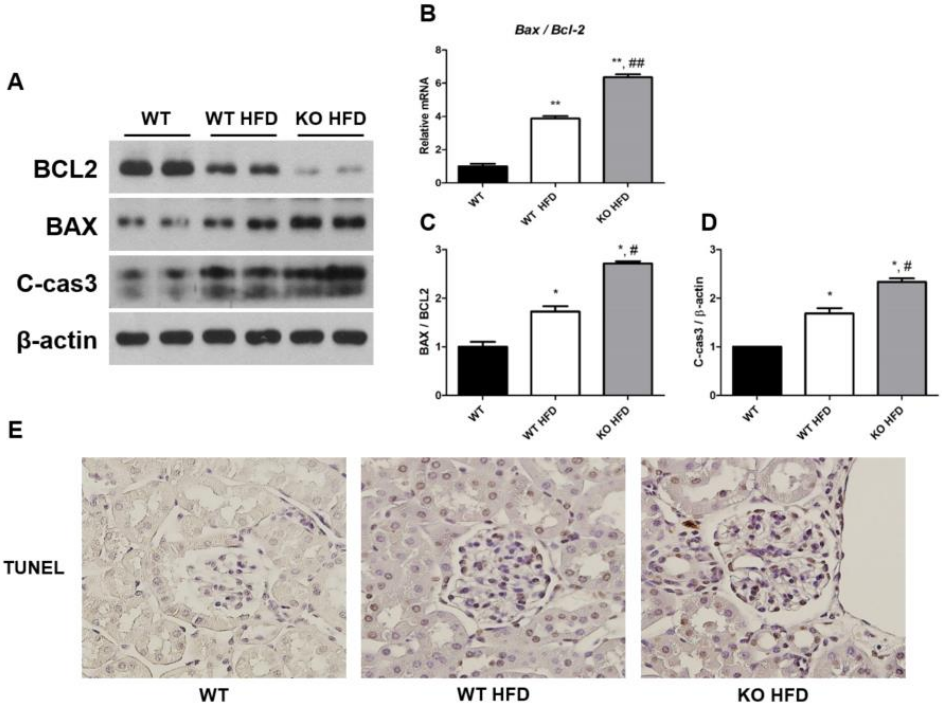

Figure 7. Decreased PCSK9 expression associates with apoptosis in DKD animal model. (A–C) The transcription and expression levels of Bax to Bcl–2 ratio of WT, WT HFD, and KO HFD animal models. **(A and D)** The expression levels of C–cas3 of experimental animal models. **(E)** TUNEL staining for the kidney samples of experimental animal models.

Note: *, $P < 0.05$ vs. WT; **, $P < 0.001$ vs. WT; #, $P < 0.05$ vs. WT HFD; ##, $P < 0.001$ vs. WT HFD.

Abbreviations: WT, wild type; HFD, high fat diet; KO, knockout; Bcl–2, B cell lymphoma–2; C–cas3, cleaved–caspase 3; TUNEL, terminal deoxynucleotidyl transferase dUTP nick–end labeling; PCSK9, proprotein convertase subtilisin/kexin type 9; DKD, diabetic kidney disease. disease.

5. The decrease of intracellular PCSK9 is associated with renal lipid accumulation in TNF–α or PA–treated mice podocytes

Preferentially I confirmed that the expression of PCSK9 gene and protein

decreased in TNF–α–treated podocyte is compared to control. The decrease in PCSK9 expression by TNF–α was alleviated when co–treated with Lv–PCSK9, while was further exacerbated when treated with siPCSK9 (**Fig. 8A–C**). It was also found that the treatment of podocyte with PA instead of TNF–α showed the same tendency as that of TNF–α (**Fig. 8D–F**).

The negative relationship between PCSK9 expression and lipid accumulation was observed by BODIPY 493/503 staining in mouse podocytes through the control of PCSK9 expression at intracellular levels using Lv–PCSK9 and siPCSK9. Lipid accumulation alleviated through an increase of PCSK9 mediated by Lv–PCSK9 but aggravated after the siPCSK9–mediated decrease in PCSK9 expression (**Fig. 9A**). Various changes in lipid accumulation induced by TNF–α treatment and PCSK9 levels in mouse podocytes were also confirmed by TEM. The accumulated lipid droplets in mouse podocytes were the most evident in the group treated with TNF–α and siPCSK9. These changes decreased in the group treated with TNF–α + Lv–PCSK9 (**Fig. 9B**). Similar results were also observed after PA treatment (**Fig. 9C and D**). In addition, cholesterol and triglyceride levels elevated by the treatment using TNF–α or PA were mitigated by PCSK9 upregulation and was further aggravated by downregulation (**Fig. 9E and F**).

Next, changes in the expression of LDLR and CD36 were observed in cell experiments as a function of PCSK9 expression. Increased expressions of LDLR and CD36 by TNF–α or PA treatment were counteracted by Lv–PCSK9 administration and was observed to be exacerbated by siPCSK9 administration (**Fig. 10**)

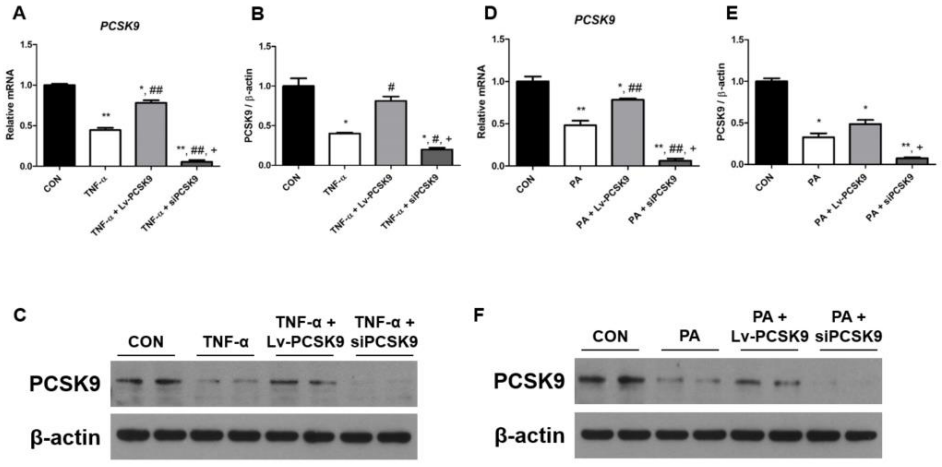

Figure 8. Changes of intracellular PCSK9 expression by TNF–α or PA treatment with intracellular PCSK9 modulation in mice podocytes. (A–C) Transcriptions (A) and expressions (B and C) of PCSK9 in podocyte treated with CON, TNF–α, TNF–α + Lv–PCSK9, and TNF–α + siPCSK9. **(D–F)** Transcriptions (D) and expressions (E and F) of PCSK9 in podocyte treated with CON, PA, PA + Lv–PCSK9, and PA + siPCSK9.

Note: *, $P < 0.05$ vs. CON; **, $P < 0.001$ vs. CON; #, $P < 0.05$ vs. TNF–α; ##, $P < 0.001$ vs. TNF–α or PA; +, $P < 0.001$ vs. TNF–α or PA + Lv–PCSK9.

Abbreviations: PCSK9, proprotein convertase subtilisin/kexin type 9; CON, control; TNF–α, tumor necrosis factor–alpha; Lv–PCSK9, CMV–mPCSK9–lentivirus; PA, palmitic acid; siPCSK9, PCSK9 siRNA.

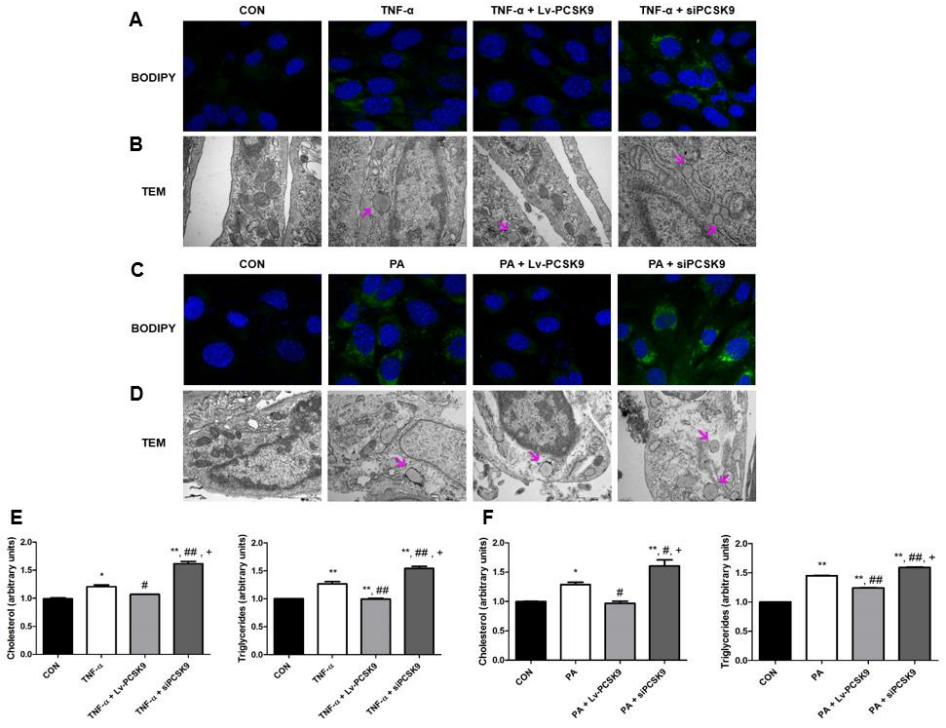

Figure 9. Decreased intracellular PCSK9 is associated with lipid accumulation in TNF–α or PA–treated mice podocytes. (A–D) BODIPY stain (A and C) and lipid droplets observed by TEM (B and D) in TNF–α or PA–treated podocytes. **(E and F)** The changes of cholesterol and triglyceride levels by PCSK9 expression in TNF–α or PA–treated podocytes.

Note: *, $P < 0.05$ vs. CON; **, $P < 0.001$ vs. CON; #, $P < 0.05$ vs. TNF–α; ##, $P < 0.001$ vs. TNF–α; +, $P < 0.001$ vs. TNF–α + Lv–PCSK9.

Abbreviations: CON, control; TNF–α, tumor necrosis factor–alpha; Lv–PCSK9, CMV–mPCSK9–lentivirus; TEM, transmission electron microscope; PA, palmitic acid; PCSK9, proprotein convertase subtilisin/kexin type 9.

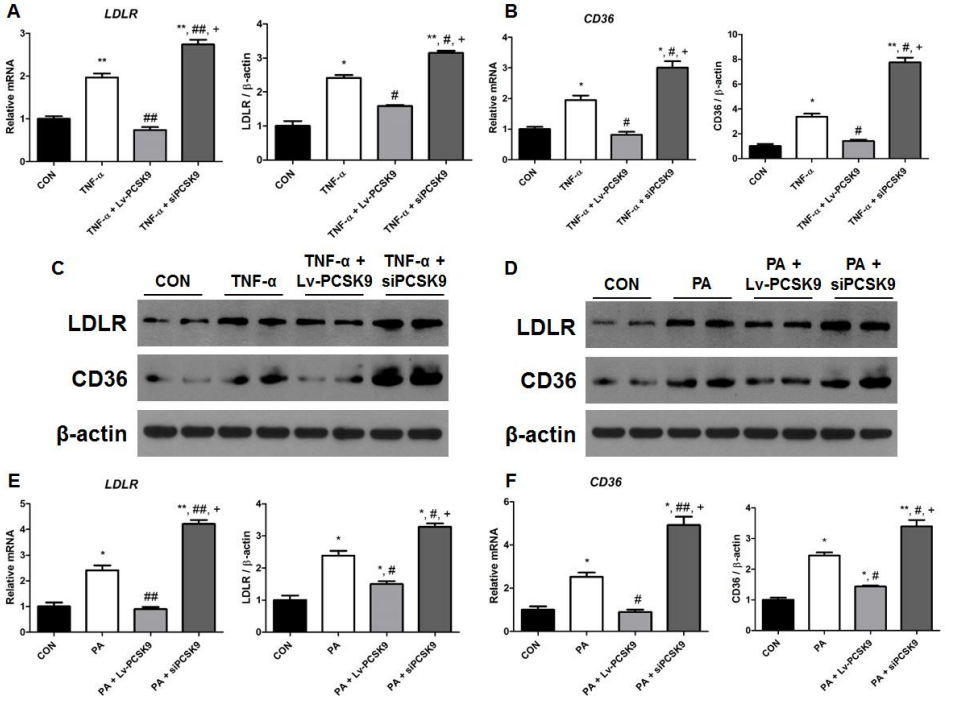

Figure 10. Decreased intracellular PCSK9 is associated with increased CD36 and LDLR expressions in TNF–α or PA–treated mice podocytes. (A–C) Changes of transcription and expression levels of LDLR and CD36 by PCSK9 expression in TNF–α–treated podocytes. **(D–F)** Changes of transcription and expression levels of LDLR and CD36 by PCSK9 expression in PA–treated podocytes.

Note: *, $P < 0.05$ vs. CON; **, $P < 0.001$ vs. CON; #, $P < 0.05$ vs. TNF–α; ##, $P < 0.001$ vs. TNF–α; +, $P < 0.001$ vs. TNF–α + Lv–PCSK9.

Abbreviations: LDLR, low–density lipoprotein cholesterol receptor; CON, control; TNF–α, tumor necrosis factor–alpha; Lv–PCSK9, CMV–mPCSK9–lentivirus; PA, palmitic acid; PCSK9, proprotein convertase subtilisin/kexin type 9.

6. Downregulated intracellular PCSK9 expression exacerbates the alteration of mitochondrial morphology and fatty acid oxidation in TNF–α

or PA–treated mice podocytes

Next, I examined how the changes in mitochondria and fatty acid oxidation due to TNF–α or PA treatment vary with PCSK9 changes *in vitro* using podocyte. Gene expression of *Ppargc1a*, *Cpt1*, and *Acox1*, was reduced by TNF–α treatment, improved by PCSK9 overexpression, but further aggravated by down–regulation (**Fig. 11A–C**). In addition, the changes in the mitochondrial morphology of the same tendency were also confirmed by TEM images (**Fig. 11D**). These alterations were in line with the treatment by PA *in vitro* (**Fig. 11E–H**).

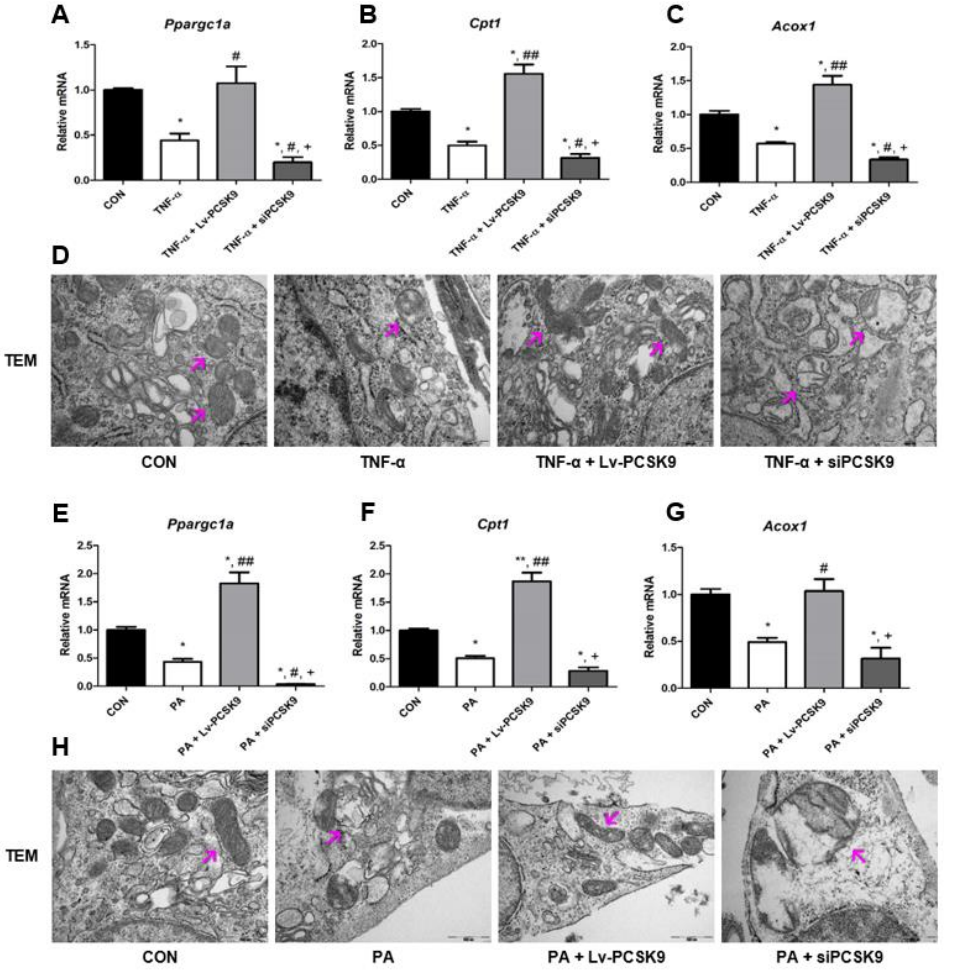

Figure 11. Downregulated intracellular PCSK9 expression is associated with mitochondrial damage and disturbed fatty acid oxidation in mice podocytes treated with TNF–α or PA. (A–C) Changes of *Ppargc1a*, *Cpt1*, and *Acox1* transcription by PCSK9 expression in TNF–α–treated podocytes. **(D)** Changes of mitochondrial morphology by PCSK9 expression in TNF–α–treated podocytes. **(E–G)** Changes of *Ppargc1a*, *Cpt1*, and *Acox1* transcription by PCSK9 expression in PA–treated podocytes. **(D)** Changes of mitochondrial morphology by PCSK9 expression in PA–treated podocytes.

Note: *, $P < 0.05$ vs. CON; **, $P < 0.001$ vs. CON; #, $P < 0.05$ vs. TNF–α or PA; ##, $P < 0.001$ vs. TNF–α or PA; +, $P < 0.001$ vs. TNF–α or PA + Lv–PCSK9.

Abbreviations: Ppargc1a, peroxisome proliferator–activated receptor gamma coactivator 1–alpha; Cpt1, carnitine palmitoyltransferase–1; Acox1, acyl–CoA oxidase; CON, control; TNF–α, tumor necrosis factor–alpha; Lv–PCSK9, CMV–mPCSK9–lentivirus; TEM, transmission electron microscope; PA, palmitic acid; PCSK9, proprotein convertase subtilisin/kexin type 9.

7. Reduction of intracellular PCSK9 expression increases apoptosis in TNF–α or PA–treated mice podocytes

Finally, I examined whether PCSK9 level changes and apoptosis are involved in podocyte treated with TNF–α or PA. The ratio of Bax to Bcl–2 gene and protein increased in TNF–α–treated podocyte compared with control, and this increase was alleviated by PCSK9 overexpression, whereas it was deteriorated by down–regulation (**Fig. 12A–C**). The same trends were also observed in gene and protein expression of cleaved–caspase 3 (**Fig. 12B and D**). Furthermore, the experiments with podocyte treated with PA were able to reaffirm the same results (**Fig. 12E–H**).

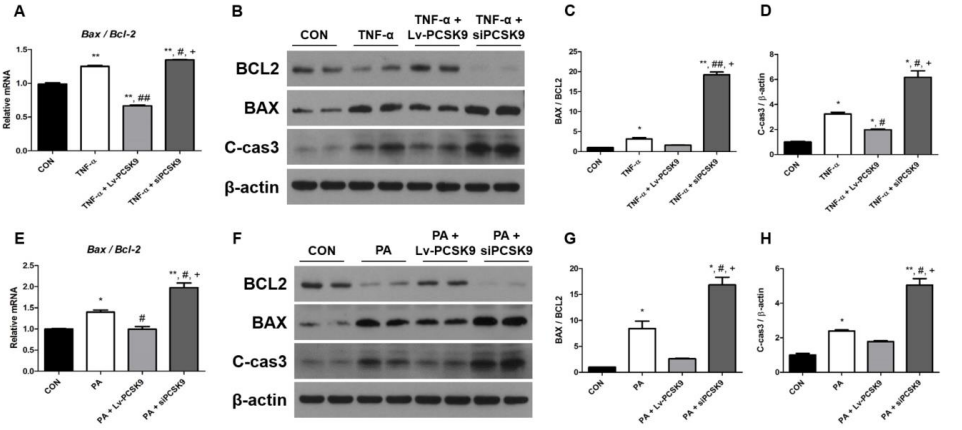

Figure 12. Downregulated intracellular PCSK9 expression is associated with apoptosis in mice podocytes treated with TNF–α or PA. (A–C) Changes of transcription and expression levels of Bax to Bcl–2 ratio by PCSK9 expression in TNF–α–treated podocytes. **(B and D)** Changes of expression levels of C–cas3 by PCSK9 expression in TNF–α–treated podocytes. Changes of transcription and expression levels of Bax to Bcl–2 ratio by PCSK9 expression in PA–treated podocytes. Changes of expression levels of C–cas3 by PCSK9 expression in PA–treated podocytes.

Note: *, $P < 0.05$ vs. CON; **, $P < 0.001$ vs. CON; #, $P < 0.05$ vs. TNF–α or PA; ##, $P < 0.001$ vs. TNF–α or PA; +, $P < 0.001$ vs. TNF–α or PA + Lv–PCSK9.

Abbreviations: CON, control; TNF–α, tumor necrosis factor–alpha; Lv–PCSK9, CMV–mPCSK9–lentivirus; Bcl–2, B cell lymphoma–2; C–cas3, cleaved–caspase 3; PA, palmitic acid; PCSK9, proprotein convertase subtilisin/kexin type 9.

IV. DISCUSSION

As is well known, PCSK9 maintains adequate circulating LDL–C levels. Although statin and other medicines have been shown to modulate circulating LDL–C levels, which have contributed greatly preventing cardiovascular

complications, it appears that these effects are not being delivered in certain individuals. Therefore, recent studies have attempted to control the circulating LDL–C levels by targeting PCSK9 in these individuals, and as a result reported positive clinical effects.[12-14] In the meantime, many studies on PCSK9 have been accumulated, but the role of PCSK9 in the kidneys has not been elucidated. In this regard, I have identified novel findings on the effects of PCSK9 on renal injury and lipid accumulation in experimental DKD models. The expression of PCSK9 has been reduced in animal and human kidney tissues with DKD. In addition, when the expression of PCSK9 was decreased in the kidney, the degree of lipid accumulation and renal injury was more severe. Furthermore, decreased renal PCSK9 was associated with aggravated mitochondrial damage and disrupted fatty acid oxidation, and its association with apoptosis was also confirmed.

Complications such as renal insufficiency have not been reported in studies using PCSK9 monoclonal antibodies,[12-14] thus it assumed that the use of PCSK9 monoclonal antibodies are not associated with renal damage.[33] However, when PCSK9 monoclonal antibody is administered, the level of free PCSK9 decreases, whereas the level of total PCSK9 shows no change or increase.[34,35] Thus, based on clinical data from the use of PCSK9 monoclonal antibody, it is difficult to conclude that the possibility of renal injury following total PCSK9 changes. Considering the difference between the reports using PCKS9 monoclonal antibody and my data which showed greatly reduced total PCSK9 expression in type 2 DKD experimental models, additional research should be accumulated on the relationship between changes in PCSK9 and renal injury.

The presence of a congenital genetic disorder, like PCKS9 loss–of–function (LOF) mutation, can affect the expression of total PCSK9. However, it is also limited to fully accept the connection point in this part. First, the four missense mutations R46L, G106R, N157K, and R237W are associated with hypocholesterolemia and possibly increased response to statin.[36,37] In addition,

people with two nonsense mutations, Y142X and C679X, had significant less incidence of coronary artery disease as well as low LDL–C levels.[38,39] However, there is no difference in circulating PCSK9 in patients with PCSK9 LOF mutation compared to the control individuals.[40] Second, PCSK9 expression in PCSK9 LOF–induced kidney cells has been showed to be highly heterogeneous.[41,42] Human kidney 2 (HK–2) cells transfected with $PCSK9^{Q152H}$ showed significantly higher levels of proPCSK9 than $PCSK9^{WT}$ cells.[41] In addition, according to the experimental report of the expression of PCSK9 in HEK 293FT cell of WT and mutant forms, 46L and 443T mutants were similar to WT, but secreted forms were significantly decreased in 253F and 679X mutants. As described previously, the phenotypes of PCSK9 LOF mutations are very diverse, and no suspected reports of renal phenotypes have been presented. On the other hand, elevated serum creatinine has been reported in human study which was administered an antisense–mediated PCSK9 inhibitor.[43] In particular, mitochondrial swelling and lysosomal aggregation were observed in renal biopsy performed in patient with acute kidney injury in the above–mentioned study.[44] Given that down–regulation of PCSK9 intensified renal injury, and overexpression attenuated this trend, changes of renal PCSK9 expression may be associated with kidney damage. Therefore, for the regulation of PCSK9 expression in the human body, clear identification of renal injury should be preceded.

Decreasing PCSK9 increases the survival of LDLR, which is likely to results in renal lipid accumulation. However, in several studies, changes in PCSK9 expression have been reported to link with lipid synthesis or efflux as well as other cell surface receptors related to influx such as fatty acid and triglyceride. First, the absence of PCSK9 resulted in the upregulation of CD36, a major receptor involved in fatty acid and triglyceride metabolism, in the liver and adipose tissue.[20] These changes result in hepatic fatty acid uptake and increased triglyceride content, which is also consistent for my results with kidneys. Second, increased PCSK9 inhibits the process of ATP–binding cassette transporter A1

(ABCA1)–mediated cholesterol efflux.[45] Third, changes in PCSK9 are closely related to sterol regulatory element–binding protein (SREBP), which plays an important role in cholesterol synthesis.[46] Thus, PCSK9 is associated with a variety of proteins that regulate lipid metabolism, expect for LDLR, and studies on the effects of PCSK9 monoclonal antibody have shown that not only LDL–C but also non–LDL–C were reduced.[12-14] Additional studies on individualized molecules involved in lipid accumulation in the future will be needed.

It is unclear whether changes of diabetic status in the KO HFD animal model affected renal injury, and the relationship between PCSK9 and diabetes is still conflicting. For this part, the first thing to consider is the possibility of diabetic deterioration following PCSK9 reduction. However, PCSK9 monoclonal antibody has been reported to be associated with diabetes mellitus or elevated blood glucose,[47,48] there also exists the report that is not related to these complications.[11] Patients with the PCSK9 loss–of–function mutation have also been reported to be associated with diabetes, which is more disorderly. The association of diabetes or hyperglycemia is thought to vary according to the type of PCSK9 loss–of–function mutation.[49-52] However, it has been reported that PCSK9–deficient animal models showed disrupted ability of insulin secretion, resulting in glucose intolerance.[53,54] Even if diabetes complications occur in the PCSK9–decreased group, the degree is not so large, thus more research is needed. Secondly, it can be considered that lipoproteins, which exhibit abnormal changes by diabetes, also affect DKD. Diabetic dyslipidemia causes a decrease in high density lipoprotein cholesterol, which leads to a decrease in cholesterol efflux.[55] In addition, the qualitative changes including increased glycated, small, dense, and oxidized LDL–C, which are preferentially impact on DKD, are greatly occurred in diabetic dyslipidemia.[56] The hypothesis that a lipid with qualitative change in DKD accelerated renal dysfunction in the PCSK9 KO model should be further validated.

Several mechanisms may be considered in relation to renal injury due to PCSK9

reduction. First, it is conceivable that renal lipid accumulation triggered by PCSK9 reduction, and which resulted in increased mitochondrial damage and apoptosis. It is well known that the occurrence of lipid accumulation and mitochondrial damage in DKD are associated with renal injury,[57] and this is consistent with my findings. Second, recent studies have shown that the C–terminal domain of PCSK9 has a different protein binding, such as amyloid precursor–like protein 2 (APLP2) or annexin 2.[58,59] In addition, the association between PCSK9 and cytokine signaling including TNF–α or activation of the Janus kinase/signal transducer and activator of transcription pathway also have been reported.[60,61] Regarding these observations, there may be a role of PCSK9 in the kidney that has not yet elucidated.

My study has some limitations. Since the animal model used in my study was the whole–body KO model of PCSK9, it is difficult to pinpoint whether the results are due to decreased PCSK9 expression in the kidney or systemic. However, the same trend can be observed in cell experiments using podocyte, thus it can be assumed that the results of this study are related to the decrease of PCSK9 expression in the kidney. Second, the effects of PCSK9 on cell expression and circulating form, respectively, were not confirmed. Because changes in circulating PCSK9 are associated with diabetes or cardiovascular outcome,[62,63] these may have served as confounders in my results. Third, although this study used an animal model that induced diabetes mellitus, there was not a clear distinction from individuals who did not develop DKD. However, there is a report that diabetes–induced animal model used in my study have characteristics of DKD,[64] and several surrogate markers suggesting DKD were identified in my data. Fourth, I did not clarify the relationship with cholesterol homeostasis–related factors, such as ABCA1 or SREBP. Since these markers can change the direction of lipid accumulation, further studies will need to clarify this part.

V. CONCLUSION

In conclusion, the renal expression of PCSK9 decreases in experimental DKD models. In addition, the decrease of PCSK9 is associated with renal lipid accumulation and injury in experimental DKD models. Furthermore, lipid accumulation and renal injury by decreased PCSK9 is associated with mitochondrial damage and apoptosis. These results suggest that PCSK9 is involved in the lipid accumulation and renal injury of DKD.

REFERENCES

1. Kimmelstiel P, Wilson C. Intercapillary Lesions in the Glomeruli of the Kidney. Am J Pathol 1936;12:83-98.7.
2. Herman-Edelstein M, Scherzer P, Tobar A, Levi M, Gafter U. Altered renal lipid metabolism and renal lipid accumulation in human diabetic nephropathy. J Lipid Res 2014;55:561-72.
3. Proctor G, Jiang T, Iwahashi M, Wang Z, Li J, Levi M. Regulation of renal fatty acid and cholesterol metabolism, inflammation, and fibrosis in Akita and OVE26 mice with type 1 diabetes. Diabetes 2006;55:2502-9.
4. Wang Z, Jiang T, Li J, Proctor G, McManaman JL, Lucia S, et al. Regulation of renal lipid metabolism, lipid accumulation, and glomerulosclerosis in FVBdb/db mice with type 2 diabetes. Diabetes 2005;54:2328-35.
5. Merscher-Gomez S, Guzman J, Pedigo CE, Lehto M, Aguillon-Prada R, Mendez A, et al. Cyclodextrin protects podocytes in diabetic kidney disease. Diabetes 2013;62:3817-27.
6. Seidah NG, Benjannet S, Wickham L, Marcinkiewicz J, Jasmin SB, Stifani S, et al. The secretory proprotein convertase neural apoptosis-regulated convertase 1 (NARC-1): liver regeneration and neuronal differentiation. Proc Natl Acad Sci U S A 2003;100:928-33.
7. Abifadel M, Rabes JP, Devillers M, Munnich A, Erlich D, Junien C, et al. Mutations and polymorphisms in the proprotein convertase subtilisin kexin 9 (PCSK9) gene in cholesterol metabolism and disease. Hum Mutat 2009;30:520-9.
8. Roche-Molina M, Sanz-Rosa D, Cruz FM, Garcia-Prieto J, Lopez S, Abia R, et al. Induction of sustained hypercholesterolemia by single adeno-associated virus-mediated gene transfer of mutant hPCSK9.

Arterioscler Thromb Vasc Biol 2015;35:50-9.

9. Denis M, Marcinkiewicz J, Zaid A, Gauthier D, Poirier S, Lazure C, et al. Gene inactivation of proprotein convertase subtilisin/kexin type 9 reduces atherosclerosis in mice. Circulation 2012;125:894-901.
10. Strom TB, Holla OL, Tveten K, Cameron J, Berge KE, Leren TP. Disrupted recycling of the low density lipoprotein receptor by PCSK9 is not mediated by residues of the cytoplasmic domain. Mol Genet Metab 2010;101:76-80.
11. Sabatine MS, Leiter LA, Wiviott SD, Giugliano RP, Deedwania P, De Ferrari GM, et al. Cardiovascular safety and efficacy of the PCSK9 inhibitor evolocumab in patients with and without diabetes and the effect of evolocumab on glycaemia and risk of new-onset diabetes: a prespecified analysis of the FOURIER randomised controlled trial. Lancet Diabetes Endocrinol 2017;5:941-50.
12. Ridker PM, Revkin J, Amarenco P, Brunell R, Curto M, Civeira F, et al. Cardiovascular Efficacy and Safety of Bococizumab in High-Risk Patients. N Engl J Med 2017;376:1527-39.
13. Robinson JG, Farnier M, Krempf M, Bergeron J, Luc G, Averna M, et al. Efficacy and safety of alirocumab in reducing lipids and cardiovascular events. N Engl J Med 2015;372:1489-99.
14. Sabatine MS, Giugliano RP, Wiviott SD, Raal FJ, Blom DJ, Robinson J, et al. Efficacy and safety of evolocumab in reducing lipids and cardiovascular events. N Engl J Med 2015;372:1500-9.
15. Lambert G, Jarnoux AL, Pineau T, Pape O, Chetiveaux M, Laboisse C, et al. Fasting induces hyperlipidemia in mice overexpressing proprotein convertase subtilisin kexin type 9: lack of modulation of very-low-density lipoprotein hepatic output by the low-density lipoprotein receptor. Endocrinology 2006;147:4985-95.
16. Herbert B, Patel D, Waddington SN, Eden ER, McAleenan A, Sun XM,

et al. Increased secretion of lipoproteins in transgenic mice expressing human D374Y PCSK9 under physiological genetic control. Arterioscler Thromb Vasc Biol 2010;30:1333-9.

17. Levy E, Ben Djoudi Ouadda A, Spahis S, Sane AT, Garofalo C, Grenier E, et al. PCSK9 plays a significant role in cholesterol homeostasis and lipid transport in intestinal epithelial cells. Atherosclerosis 2013;227:297-306.
18. Rashid S, Tavori H, Brown PE, Linton MF, He J, Giunzioni I, et al. Proprotein convertase subtilisin kexin type 9 promotes intestinal overproduction of triglyceride-rich apolipoprotein B lipoproteins through both low-density lipoprotein receptor-dependent and -independent mechanisms. Circulation 2014;130:431-41.
19. Roubtsova A, Munkonda MN, Awan Z, Marcinkiewicz J, Chamberland A, Lazure C, et al. Circulating proprotein convertase subtilisin/kexin 9 (PCSK9) regulates VLDLR protein and triglyceride accumulation in visceral adipose tissue. Arterioscler Thromb Vasc Biol 2011;31:785-91.
20. Demers A, Samami S, Lauzier B, Des Rosiers C, Ngo Sock ET, Ong H, et al. PCSK9 Induces CD36 Degradation and Affects Long-Chain Fatty Acid Uptake and Triglyceride Metabolism in Adipocytes and in Mouse Liver. Arterioscler Thromb Vasc Biol 2015;35:2517-25.
21. Ding Z, Liu S, Wang X, Mathur P, Dai Y, Theus S, et al. Cross-Talk Between PCSK9 and Damaged mtDNA in Vascular Smooth Muscle Cells: Role in Apoptosis. Antioxid Redox Signal 2016;25:997-1008.
22. Wu CY, Tang ZH, Jiang L, Li XF, Jiang ZS, Liu LS. PCSK9 siRNA inhibits HUVEC apoptosis induced by ox-LDL via Bcl/Bax-caspase9-caspase3 pathway. Mol Cell Biochem 2012;359:347-58.
23. Cohen CD, Frach K, Schlondorff D, Kretzler M. Quantitative gene expression analysis in renal biopsies: a novel protocol for a high-throughput multicenter application. Kidney Int 2002;61:133-40.

24. Berthier CC, Zhang H, Schin M, Henger A, Nelson RG, Yee B, et al. Enhanced expression of Janus kinase-signal transducer and activator of transcription pathway members in human diabetic nephropathy. Diabetes 2009;58:469-77.
25. Srinivasan K, Viswanad B, Asrat L, Kaul CL, Ramarao P. Combination of high-fat diet-fed and low-dose streptozotocin-treated rat: a model for type 2 diabetes and pharmacological screening. Pharmacol Res 2005;52:313-20.
26. Reed MJ, Meszaros K, Entes LJ, Claypool MD, Pinkett JG, Gadbois TM, et al. A new rat model of type 2 diabetes: the fat-fed, streptozotocin-treated rat. Metabolism 2000;49:1390-4.
27. Mundel P, Reiser J, Zuniga Mejia Borja A, Pavenstadt H, Davidson GR, Kriz W, et al. Rearrangements of the cytoskeleton and cell contacts induce process formation during differentiation of conditionally immortalized mouse podocyte cell lines. Exp Cell Res 1997;236:248-58.
28. Lois C, Refaeli Y, Qin XF, Van Parijs L. Retroviruses as tools to study the immune system. Curr Opin Immunol 2001;13:496-504.
29. Nam BY, Kim DK, Park JT, Kang HY, Paeng J, Kim S, et al. Double transduction of a Cre/LoxP lentiviral vector: a simple method to generate kidney cell-specific knockdown mice. Am J Physiol Renal Physiol 2015;309:F1060-9.
30. Kang SW, Adler SG, Lapage J, Natarajan R. p38 MAPK and MAPK kinase 3/6 mRNA and activities are increased in early diabetic glomeruli. Kidney Int 2001;60:543-52.
31. Yoo TH, Pedigo CE, Guzman J, Correa-Medina M, Wei C, Villarreal R, et al. Sphingomyelinase-like phosphodiesterase 3b expression levels determine podocyte injury phenotypes in glomerular disease. J Am Soc Nephrol 2015;26:133-47.
32. Han SH, Wu MY, Nam BY, Park JT, Yoo TH, Kang SW, et al. PGC-

1alpha Protects from Notch-Induced Kidney Fibrosis Development. J Am Soc Nephrol 2017;28:3312-22.

33. Toth PP, Dwyer JP, Cannon CP, Colhoun HM, Rader DJ, Upadhyay A, et al. Efficacy and safety of lipid lowering by alirocumab in chronic kidney disease. Kidney Int 2018;93:1397-408.

34. Ni YG, Di Marco S, Condra JH, Peterson LB, Wang W, Wang F, et al. A PCSK9-binding antibody that structurally mimics the EGF(A) domain of LDL-receptor reduces LDL cholesterol in vivo. J Lipid Res 2011;52:78-86.

35. Zhang L, McCabe T, Condra JH, Ni YG, Peterson LB, Wang W, et al. An anti-PCSK9 antibody reduces LDL-cholesterol on top of a statin and suppresses hepatocyte SREBP-regulated genes. Int J Biol Sci 2012;8:310-27.

36. Berge KE, Ose L, Leren TP. Missense mutations in the PCSK9 gene are associated with hypocholesterolemia and possibly increased response to statin therapy. Arterioscler Thromb Vasc Biol 2006;26:1094-100.

37. Kotowski IK, Pertsemlidis A, Luke A, Cooper RS, Vega GL, Cohen JC, et al. A spectrum of PCSK9 alleles contributes to plasma levels of low-density lipoprotein cholesterol. Am J Hum Genet 2006;78:410-22.

38. Cohen J, Pertsemlidis A, Kotowski IK, Graham R, Garcia CK, Hobbs HH. Low LDL cholesterol in individuals of African descent resulting from frequent nonsense mutations in PCSK9. Nat Genet 2005;37:161-5.

39. Cohen JC, Boerwinkle E, Mosley TH, Jr., Hobbs HH. Sequence variations in PCSK9, low LDL, and protection against coronary heart disease. N Engl J Med 2006;354:1264-72.

40. Ooi TC, Krysa JA, Chaker S, Abujrad H, Mayne J, Henry K, et al. The Effect of PCSK9 Loss-of-Function Variants on the Postprandial Lipid and ApoB-Lipoprotein Response. J Clin Endocrinol Metab 2017;102:3452-60.

41. Lebeau P, Platko K, Al-Hashimi AA, Byun JH, Lhotak S, Holzapfel N, et al. Loss-of-function PCSK9 mutants evade the unfolded protein response sensor GRP78 and fail to induce endoplasmic reticulum stress when retained. J Biol Chem 2018;293:7329-43.
42. Zhao Z, Tuakli-Wosornu Y, Lagace TA, Kinch L, Grishin NV, Horton JD, et al. Molecular characterization of loss-of-function mutations in PCSK9 and identification of a compound heterozygote. Am J Hum Genet 2006;79:514-23.
43. van Poelgeest EP, Hodges MR, Moerland M, Tessier Y, Levin AA, Persson R, et al. Antisense-mediated reduction of proprotein convertase subtilisin/kexin type 9 (PCSK9): a first-in-human randomized, placebo-controlled trial. Br J Clin Pharmacol 2015;80:1350-61.
44. van Poelgeest EP, Swart RM, Betjes MG, Moerland M, Weening JJ, Tessier Y, et al. Acute kidney injury during therapy with an antisense oligonucleotide directed against PCSK9. Am J Kidney Dis 2013;62:796-800.
45. Adorni MP, Cipollari E, Favari E, Zanotti I, Zimetti F, Corsini A, et al. Inhibitory effect of PCSK9 on Abca1 protein expression and cholesterol efflux in macrophages. Atherosclerosis 2017;256:1-6.
46. Jeong HJ, Lee HS, Kim KS, Kim YK, Yoon D, Park SW. Sterol-dependent regulation of proprotein convertase subtilisin/kexin type 9 expression by sterol-regulatory element binding protein-2. J Lipid Res 2008;49:399-409.
47. Ference BA, Robinson JG, Brook RD, Catapano AL, Chapman MJ, Neff DR, et al. Variation in PCSK9 and HMGCR and Risk of Cardiovascular Disease and Diabetes. N Engl J Med 2016;375:2144-53.
48. de Carvalho LSF, Campos AM, Sposito AC. Proprotein Convertase Subtilisin/Kexin Type 9 (PCSK9) Inhibitors and Incident Type 2 Diabetes: A Systematic Review and Meta-analysis With Over 96,000

Patient-Years. Diabetes Care 2018;41:364-7.

49. Bonnefond A, Yengo L, Le May C, Fumeron F, Marre M, Balkau B, et al. The loss-of-function PCSK9 p.R46L genetic variant does not alter glucose homeostasis. Diabetologia 2015;58:2051-5.

50. Chikowore T, Cockeran M, Conradie KR, van Zyl T. C679X loss-of-function PCSK9 variant lowers fasting glucose levels in a black South African population: A longitudinal study. Diabetes Res Clin Pract 2018;144:279-85.

51. Li AH, Morrison AC, Kovar C, Cupples LA, Brody JA, Polfus LM, et al. Analysis of loss-of-function variants and 20 risk factor phenotypes in 8,554 individuals identifies loci influencing chronic disease. Nat Genet 2015;47:640-2.

52. Saavedra YGL, Dufour R, Baass A. Familial hypercholesterolemia: PCSK9 InsLEU genetic variant and prediabetes/diabetes risk. J Clin Lipidol 2015;9:786-93.e1.

53. Da Dalt L, Ruscica M, Bonacina F, Balzarotti G, Dhyani A, Di Cairano E, et al. PCSK9 deficiency reduces insulin secretion and promotes glucose intolerance: the role of the low-density lipoprotein receptor. Eur Heart J 2019;40:357-68.

54. Mbikay M, Sirois F, Mayne J, Wang GS, Chen A, Dewpura T, et al. PCSK9-deficient mice exhibit impaired glucose tolerance and pancreatic islet abnormalities. FEBS Lett 2010;584:701-6.

55. Orekhov AN, Pushkarsky T, Oishi Y, Nikiforov NG, Zhelankin AV, Dubrovsky L, et al. HDL activates expression of genes stimulating cholesterol efflux in human monocyte-derived macrophages. Exp Mol Pathol 2018;105:202-7.

56. Verges B. Pathophysiology of diabetic dyslipidaemia: where are we? Diabetologia 2015;58:886-99.

57. Schrauwen P, Hesselink MK. Oxidative capacity, lipotoxicity, and

mitochondrial damage in type 2 diabetes. Diabetes 2004;53:1412-7.

58. DeVay RM, Shelton DL, Liang H. Characterization of proprotein convertase subtilisin/kexin type 9 (PCSK9) trafficking reveals a novel lysosomal targeting mechanism via amyloid precursor-like protein 2 (APLP2). J Biol Chem 2013;288:10805-18.

59. Mayer G, Poirier S, Seidah NG. Annexin A2 is a C-terminal PCSK9-binding protein that regulates endogenous low density lipoprotein receptor levels. J Biol Chem 2008;283:31791-801.

60. Cao A, Wu M, Li H, Liu J. Janus kinase activation by cytokine oncostatin M decreases PCSK9 expression in liver cells. J Lipid Res 2011;52:518-30.

61. Ruscica M, Ricci C, Macchi C, Magni P, Cristofani R, Liu J, et al. Suppressor of Cytokine Signaling-3 (SOCS-3) Induces Proprotein Convertase Subtilisin Kexin Type 9 (PCSK9) Expression in Hepatic HepG2 Cell Line. J Biol Chem 2016;291:3508-19.

62. Eisenga MF, Zelle DM, Sloan JH, Gaillard C, Bakker SJL, Dullaart RPF. High Serum PCSK9 Is Associated With Increased Risk of New-Onset Diabetes After Transplantation in Renal Transplant Recipients. Diabetes Care 2017;40:894-901.

63. Leander K, Malarstig A, Van't Hooft FM, Hyde C, Hellenius ML, Troutt JS, et al. Circulating Proprotein Convertase Subtilisin/Kexin Type 9 (PCSK9) Predicts Future Risk of Cardiovascular Events Independently of Established Risk Factors. Circulation 2016;133:1230-9.

64. Sugano M, Yamato H, Hayashi T, Ochiai H, Kakuchi J, Goto S, et al. High-fat diet in low-dose-streptozotocin-treated heminephrectomized rats induces all features of human type 2 diabetic nephropathy: a new rat model of diabetic nephropathy. Nutr Metab Cardiovasc Dis 2006;16:477-84.

ABSTRACT (IN KOREAN)

PCSK9이 당뇨병성 신증에서 사구체 지질 축적 및 신손상에 미치는 영향

< 지도교수 유 태 현 >

연세대학교 대학원 의학과

윤 창 연

배경: 사구체 지질 축적은 당뇨병성 신증의 병리학적인 특징 가운데 하나이다. 최근 연구를 통해 proprotein convertase subtilisin/kexin type 9 (PCSK9)이 세포 지질 조절에 중요한 역할을 하는 것으로 알려지고 있다.

목적: 본 연구를 통하여 당뇨병성 신증에서 PCSK9이 사구체 및 족세포 지질 축적 및 손상 과정에 어떠한 역할을 하는지 알아보고자 하였다.

방법: C57BL/6와 PCSK9 발현을 제거한 쥐에게 고지방식이 및 12주간의 저농도 streptozotocin 복강내 투여를 통하여 2형 당뇨를 유발하였다. 신장내 지질 축적은 BODIPY 493/503 염색을 통하여 확인하였다. 쥐 족세포를 이용한 다양한 자극 실험에서 PCSK9 발현의 증가 및 저하에 대한 조절은 lentivirus 또는 small-interfering RNA (siRNA)를 통하여 진행하였다. 세포사멸, 미토콘드리아 형태 변화, 및 에너지 대사와 관련된 주요 인자들의 변화를 체내 및 체외 실험을 통하여 확인하였다.

결과: 대조군이나 당뇨병성신증을 가지고 있는 쥐에 비하여 PCSK9 발현이 제거된 당뇨병성신증 쥐의 신장에서 지질 축적의 증가가 관찰되었다. 또한, PCSK9 발현이 제거된 쥐에서 미토콘드리아 모양과 에너지 대사와 관련된 단백질들의 변형이 관찰되었다. 족세포를 이용한 세포 실험에서 당뇨 자극에 의하여 미토콘드리아의 팽창 및 파괴 소견이 동반된 세포내 지질 축적 및 세포사멸 소견이 관찰되었다. 이러한 변화들은 PCSK9 발현을 증가시키는 경우 호전되었고, siRNA로 발현을 감소시키는 경우 악화되었다.

결론: 이상의 결과를 종합하여 볼 때, 당뇨병성 신증에서 족세포의 PCSK9 발현 감소는 미토콘드리아의 손상 및 세포사멸을 통하여 지질 축적과 신손상을 일으키는 것에 관여하는 것으로 생각된다.

핵심되는 말: PCSK9, 지질 축적, 족세포, 미토콘드리아, 당뇨병성신증